Veterinary Microbiology 235 (2019) 199–208

Contents lists available at ScienceDirect

Veterinary Microbiology

journal homepage: www.elsevier.com/locate/vetmic

MTOR involved in bacterial elimination against *Trueperella pyogenes* infection based on mice model by transcriptome and biochemical analysis

Ting Huang[a,b,1], Kai Cui[b,1], Xuhao Song[b], Jie Jing[b], Jiafu Lin[a], Xinrong Wang[a], Xiuyue Zhang[b], Yiwen Chu[a,*], Bisong Yue[c,*]

[a] Antibiotics Research and Re-evaluation Key Laboratory of Sichuan Province, SichuanIndustrial Institute of Antibiotics, Chengdu University, Chengdu, China
[b] Key Laboratory of Bio-resources and Eco-environment (Ministry of Education), College of Life Sciences, Sichuan University, Chengdu, China
[c] Sichuan Key Laboratory of Conservation Biology on Endangered Wildlife, College of Life Sciences, Sichuan University, Chengdu, China

ARTICLE INFO

Keywords:
Trueperella pyogenes
Transcriptome
Differentially expressed genes
mTOR autophagy
Bacterial elimination

ABSTRACT

Trueperella pyogenes is an importantly opportunistic and commensal pathogen that causes suppurative lesions of most economically important livestock. To understand the molecular mechanism underlying the infection by *T. pyogenes*, we carried out a large-scale transcriptome sequencing of mice livers intraperitoneally infected with *T. pyogenes* using RNA-sequencing. A total of 47 G clean bases were obtained and 136 differentially expressed genes were detected between the control and the infection groups in the liver transcriptomes. Additionally, we found that the expression of a key autophagy regulator, mTOR (mechanistic target of rapamycin) was significantly up-regulated in the infection groups. Mechanistically, *T. pyogenes* infection induced the expression of mTOR and subsequently inhibited the autophagy of host cell. Blocking autophagy with inhibitor 3-methyladenine (3-MA) or silencing autophagy-related gene 7 (Atg7) reduced the effect of bacterial elimination. Interestingly, inhibition of mTOR induced autophagy and reduced *T. pyogenes* viability in RAW264.7 murine macrophages. The silencing mTOR regulated oxidation and cytokines (interleukin-1β, IL-6 and tumor necrosis factro-α) against *T. pyogenes* in macrophages and significantly protected mice from *T. pyogenes* challenge. These findings indicate that mTOR is a novel functional regulator in autophagy-mediated *T. pyogenes* elimination and will be useful to further knowledge on the development of effective therapeutic strategy to control *T. pyogenes*-related diseases.

1. Introduction

Trueperella pyogenes is a versatile and opportunistic Gram-positive bacterium (Jost and Billington, 2005; Ribeiro et al., 2015), which is found on the skin, endometrium, upper respiratory, or gastrointestinal tracts of economically important livestock (Amos et al., 2014; Ribeiro et al., 2015). The bacterium can invade the blood stream of host, causing abscesses and suppurative lesions in a variety of organs and tissues (Haritani et al., 1990). In addition, *T. pyogenes* is the most significant pathogen in the formation of abscesses such as liver abscesses in the endangered forest musk deer (*Moschus berezovskii*), which is protected by Chinese legislation due to its declining population numbers (Huang et al., 2016; Zhao et al., 2011). Although research has progressed in understanding musk deer abscesses over the past decade (Zhao et al., 2017, 2011; Zhao et al., 2013), the molecular mechanism of the host response to *T. pyogenes* infection remains largely unknown. Therefore, it is urgently needed to explore the molecular mechanism underlying the pathogenesis caused by *T. pyogenes* for the treatment and control of *T. pyogenes* infection.

To achieve this goal, it is critical to investigate the interaction between the host transcriptional responses and simultaneous pathogen during the infection. Numerous researches have determined the interaction dynamics between pathogens and hosts using RNA sequencing (RNA-seq), which is a rapidly developing and effective approach to analyze transcriptomes (Martin and Wang, 2011; Zhou et al., 2016). For instance, researchers observed that *Pseudomonas aeruginosa* infection significantly triggered a pro-inflammatory response in murine model using RNA-seq (Damron et al., 2016). These investigations provide a global view of the transcriptional changes and molecular mechanisms between pathogens and host immune defense response. Autophagy is a very conserved cellular self-digestion and catabolism pathway to degrade the denatured proteins, senescent or damaged organelles in the

Abbreviations: Ctrl, Controlled samples; TP, *T. pyogenes* infected samples

* Corresponding authors.
E-mail addresses: chuyiwen@cdu.edu.cn (Y. Chu), bsyue@scu.edu.cn (B. Yue).

[1] These authors contributed equally to this work.

https://doi.org/10.1016/j.vetmic.2019.06.021
Received 23 May 2019; Received in revised form 18 June 2019; Accepted 24 June 2019

cytoplasm (Yang and Klionsky, 2010). Particularly, autophagy also plays the key roles in cellular homeostasis, responding to pathogen invasion or elimination (Gomes and Dikic, 2014). The dysregulation of autophagy is responsible for many pathogenic infections, implying the significance of its precise control (Deretic et al., 2013). The mTOR (mechanistic target of rapamycin) is an important component which could regulate autophagy to respond the cellular physiological conditions or different environmental stress (Jung et al., 2010). Recently, several investigations have established that mTOR functions as an important regulator in the manipulation of immune related genes in response to pathogen infection (Foldenauer et al., 2013; Liu et al., 2017).

In the current study, to identify the key genes and molecular events involved in *T. pyogenes* infection, we first performed transcriptome sequencing of mice livers. We found that *T. pyogenes* infection induced the expression of mTOR and inhibiting mTOR significantly reduced *T. pyogenes* viability *in vitro* and *in vivo*, suggesting mTOR as a novel functional regulator involved in bacterial elimination responses with *T. pyogenes* infection. This research will facilitate understanding of the molecular mechanism of the host response to *T. pyogenes* invasion at the transcriptional level and may lead to the development of effective therapeutic strategies to combat *T. pyogenes* infection.

2. Materials and methods

2.1. Bacterial strains, cells, plasmids and siRNA

The *T. pyogenes* stains TP13, TP7 and TP8 were isolated from *M. berezovskii* (Zhao et al., 2014, 2011) and identified as previously described (Zhao et al., 2011). These strains were cultivated on agar medium containing 5% fetal bovine serum (FBS) at 37 ℃ with 5% CO_2. The RAW264.7 murine macrophages were grown in Dulbecco's Modified Essential Medium (DMEM) containing 10% FBS at 37 ˚C with 5% CO_2. The pcDNA3-Au-mTOR-Wild type plasmids was a gift from Dr. Fuyuhiko Tamanoi (Addgene plasmid #26036) (Sato et al., 2010). The MTOR or ATG7 siRNA and scrambled negative control (NC) siRNA were obtained from Santa Cruz Biotechnology (Santa Cruz, USA).

2.2. Mice and peritoneal infection model

The out-bred specific-pathogen-free (SPF) female Kunming (KM) mice were purchased from Dashuo Biotechnology (Chengdu, China) at 10–12 weeks of age. The KM mice were randomly divided into 2 groups (8 mice per group), which were Control-Liver group and Infection-Liver group. The infection experiments were performed as described previously by the published reports (Huang et al., 2018b). Briefly, the *T. pyogenes* TP8 stain was adjusted to 1.0×10^8 colony forming units (CFU)/ml in phosphate buffered saline (PBS, pH 7.4). After anesthetizing with ketamine (40 mg/kg), the Infection-Liver group of mice were challenged with 3.7×10^7 CFU *T. pyogenes* TP8 by intraperitoneal injection. Likewise, the Control-Liver group of mice were treated with 50 μl PBS. The mice were euthanized ˜24 h post-infection, the livers and peritoneal fluid (PF) of two groups' treated mice were aseptically harvested. The CFU assay was performed to confirm the success of the infection by detecting the bacterial burdens of livers and PF as previously described (Huang et al., 2016). The total RNA was isolated from the livers samples by using TRIzol reagent (Invitrogen, Carlsbad, USA) following the manufacturer's instructions. All animal protocols were performed in accordance with the Institutional Animal Care and Use Committee guidelines of Sichuan University.

2.3. Transcriptome analysis

The complementary DNA libraries were obtained and sequenced by using Illumina Hiseq 4000 platform according to a previous report (Liu et al., 2015). After removing the low-quality reads, reads of each sample ware aligned to the mouse genome by using hisat2 with default parameters. The expression level of each sample was estimated and normalized to RPKM (reads per kilo base per million) by Stringtie assembler (Pertea et al., 2015). The Pearson's correlation coefficients (R) analysis was performed to analyze the correlations between control and treated groups in each two replicates. To identify the DEGs from the two groups under different treatment, the abundance of genes was counted by Stringtie. DEGs with p-value < 0.01 were produced by Ballgown software (Pertea et al., 2016). The DEGs of liver group were entered into the Gene Ontology (GO) and Kyoto Encyclopedia of Genes and Genomes (KEGG) pathway enrichment functional analysis using the GO database (Young et al., 2010) and KEGG database (http://www.genome.jp/kegg/). To further analyze the DEGs data of mice tissues, hierarchical clustering and PPI (protein-protein interaction) networks was applied according to the previously reports (Kolde, 2015; Saito et al., 2012).

2.4. Quantitative PCR (qPCR)

The qPCR experiment was performed to validate those DEGs identified above. Specific primers (Table S1) were designed by using Primer Premier 6.0 software, based on the sequences from the GenBank. The total RNA from the mice livers were extracted by using animal total RNA isolation kit (Foregene, Chengdu, China), followed by reverse transcription and qPCR using a One-Step qRT-PCR kit (TransGen, Beijing, China) in accordance with the manufacturer's instructions. The qPCR experiments were performed in triplicate. Gene expression was analyzed using the $2^{-\Delta CT}$ method and was normalized to *β-actin* levels in each sample.

2.5. Western blotting analysis

The mouse monoclonal antibodies (Abs) against GAPDH (Cat #sc-137179), mTOR (Cat #sc-517464), and LC-3 (Cat #sc-398822) were purchased from Santa Cruz Biotechnology (Santa Cruz). The cell samples were lysed in RIPA buffer and separated by electrophoresis on 14% SDS-PAGE gels and subsequently transferred to nitrocellulose (GE Amersham Biosciences, Piscataway, USA). Proteins were detected by western blotting using primary Abs and the relevant secondary Abs conjugated to Horseradish peroxidase (HRP) (Cat #sc-516102, Santa Cruz). The ECL reagents were used for exposure (Sigma-Aldrich, St Louis, USA) (Huang et al., 2018a).

2.6. Confocal microscopy

The RAW264.7 cells were transfected by using NC siRNA or mTOR siRNA for 24 h–48 h following the manufacturer's instructions. Cells were treated with TP8 at a multiplicity of infection (MOI) of 10:1 for 6 h, incubated with primary mouse anti-LC3 Abs and the second goat anti-mouse IgG-FITC (fluorescein isothiocyanate) Abs (Santa Cruz) as previously described (Huang et al., 2018a). The nucleus was stained by 4′,6-diamidino-2-phenylindole (DAPI) (Sigma-Aldrich). The fluorescence signals were detected by confocal microscopy (Leica, Germany) (Huang et al., 2016).

2.7. MTT assay

To investigate the impact of mTOR inhibition on cell survival, the RAW264.7 cells was collected after treatment with NC siRNA or mTOR siRNA. The cell survival was detected by the 3-(4,5-dimethylthiazol-2-yl)-2,5-diphenyltetrazolium bromide (MTT) assay according to a previous report (Preta et al., 2015).

2.8. Enzyme-linked immune-sorbent assay (ELISA)

To estimate relative cytokine levels in RAW264.7 cells, the suspension of the cells was collected with 1 ml of PBS after treatment with

NC siRNA or mTOR siRNA. The cytokine levels of tumour necrosis factor α (TNF-α), interleukin (IL)-1β, and IL-6 were measured using a ELISArray Kit (ChengLinBio, China) according to the manufacturer's instructions (Huang et al., 2018b).

2.9. Oxidation assays

To study the impact of mTOR inhibition on cell oxidation, the RAW264.7 cells was collected after treatment with PBS (control) or rapamycin (Cat #553210, Sigma-Aldrich). Nitroblue tetrazolium assay, dihydrodichlorofluorescein diacetate (H_2DCF) assay and mitochondrial membrane potential (JC-1) assay were performed according to the manufacturer's instructions, respectively (Li et al., 2015b).

2.10. Mice survivability and histological analysis

The KM mice were randomly divided into 2 groups (8 mice per group), which were Ctrl-siRNA group and mTOR-siRNA group. The Ctrl-siRNA group and mTOR-group mice were intravenously injected with 50 μl control or mTOR siRNA twice in 2 days and then intraperitoneally challenged with 3.7×10^7 CFU *T. pyogenes* TP8. The bacterial burdens of liver and PF, or the survival rate of the challenged mice were monitored for the subsequent two weeks as previously described (Huang et al., 2018b). After the necropsy, the livers of two groups' mice were aseptically harvested and fixed in 8% formalin. The paraffin-embedded tissue sections were prepared and were stained with hematoxylin-eosin (Huang et al., 2018a). All the sections were done by triplicates and examined by light microscopy.

2.11. Statistical analysis

Data and statistical tests were analyzed using Graphpad Prism 6.0. Means were compared by using a one-way analysis of variance (ANOVA) and followed by a Tukey-Kramer *post hoc* test using a 95% confidence interval. A Mantel-Cox log rank test was used to compare the survival rates between mTOR siRNA-treated mice and the NC siRNA-treated group. Differences were considered significant at $p < 0.05$.

3. Results

3.1. Comparative transcriptome analysis

One non-normalized library was constructed using *T. pyogenes* infected tissue with normal tissue as control, to obtain the liver transcriptome expression profiles of mice with *T. pyogenes* infection. The infection efficiency was confirmed by the CFU assay (Fig. S1A and B). The resulting Pearson's correlation coefficients (R) were shown in Fig. S1C and D. Illumina sequencing data from mice were deposited in Genbank under accessions, PRJNA392959. A total of 158,927,359 Illumina PE raw reads were obtained (Table 1). To better investigate the biological mechanism of host response to bacterial infection, it is important to identify the DEGs between uninfected and infected samples. A total of 136 DEGs were identified in the *T. pyogenes* infected tissue compared to normal mice tissue, including 70 up-regulated genes and 66 down-regulated genes in the livers (Table S2). GO assignments were performed to analyze the functions of these DEGs. We found that 136 DEGs in the livers encoded 366 proteins and 304 proteins were assigned to GO terms (Fig. 1A). Hierarchical clustering analysis was performed for the DEGs after extracting the expression values of the DEGs. The results showed that the DEGs clearly distinguished the *T. pyogenes* treated samples from the normal mice samples (Fig. 1B). Forty PPI pairs were identified by submitting the DEGs to the STRING database. As shown in Fig.1C, the PPI network had 39 nodes (representing proteins encoded by the DEGs) and Ppp2ca (degree = 6), Rps19 (degree = 5), Mrps2 (degree = 4), Jak3 (degree = 4), Mtor (degree = 6) had higher degrees and betweenness values. DEGs were mapped to the reference pathway in the KEGG database to identify the defending biological pathway during the infection process. The results showed that a total of 11 signal pathways were predicted in *T. pyogenes* infected liver (Table S3). Although a slightly greater number of transcripts were associated with signal transduction than immune system, most of the pathways in signal transduction are presented in liver and play an important role in the immune system. The annotated immune pathways contain more than 70% mapped genes of the total number of known genes in the pathway. Thus, *T. pyogenes* infection might impair immunity by regulating the expression of immune-related genes. Next, we selected 12 immune-related genes from the annotated immune pathways such as PI3K-Akt, Jak-STAT, and mTOR signaling pathway which were significantly affected by *T. pyogenes* infection. The relative expression levels of 12 subject genes were examined to confirm the expression profile data in the liver group (Fig. 1D) by qPCR. Ten genes exhibited > 2 folds higher expression in the mice in response to *T. pyogenes* infection and mTOR is highly expressed compared to other 11 genes. Given that mTOR is significantly expressed in liver transcriptome and is a key regulator of autophagy, we focus on mTOR and further investigate its roles throughout this study.

3.2. The inhibition of mTOR induced autophagy and reduced bacterial burdens in macrophages

To study whether autophagy induction could reduce *T. pyogenes* burdens in macrophages by regulating mTOR, RAW264.7 cells were infected with *T. pyogenes* TP8 and then treated with rapamycin, a well-known autophagy inducer. The results showed that bacterial CFU was decreased significantly in the RAW264. 7 cells compared to control group (Fig. 2A). These findings were further confirmed by using another isolates such as highly virulent isolate *T. pyogenes* TP7 and lowly virulent isolate *T. pyogenes* TP13. In addition, qPCR analysis (Fig. 2B) indicated that rapamycin significantly reduced mTOR expression and induced LC3 expression in RAW264.7 cells following *T. pyogenes* infection. These results were further confirmed by evaluated the activity of mTOR by quantifying mTOR targets such as S6K1 and 4EBP1 (Lee et al., 2007) (Fig. 2C). Although *T. pyogenes* infection had effects on cell survival of RAW264. 7 cells, treatment with rapamycin protected cells against *T. pyogenes* (Fig. 2D). Interestingly, blocking autophagy with autophagy-related gene 7 (ATG7) siRNA (Fig. 2E) or inhibitor 3-methyladenine (3-MA) (Fig. 2F) partially reversed these effects with

Table 1
Summary of sequences analysis.

Samples	Raw Reads (bp)	Clean Reads (bp)	Clean Bases (G)	Q20 (%)	Q30 (%)	GC (%)	Mapping rate (%)
Ctrl- Liver1	32,961,396	32,345,081	9.7	97.22	93.10	47.86	96.56
Ctrl- Liver2	39,847,174	39,467,721	11.84	95.47	88.88	49.43	93.82
TP-Liver1	36,573,451	35,761,560	10.73	97.67	93.97	48.83	97.00
TP-Liver2	49,454,338	49,105,950	14.73	94.92	87.84	49.34	93.25
Total	158,927,359	156,680,312	47				

Abbreviation: Ctrl: Control samples. TP: *T. pyogenes* infected samples. Q20: The percentage of bases with a Phred value > 20. Q30: The percentage of bases with a Phred value > 30.

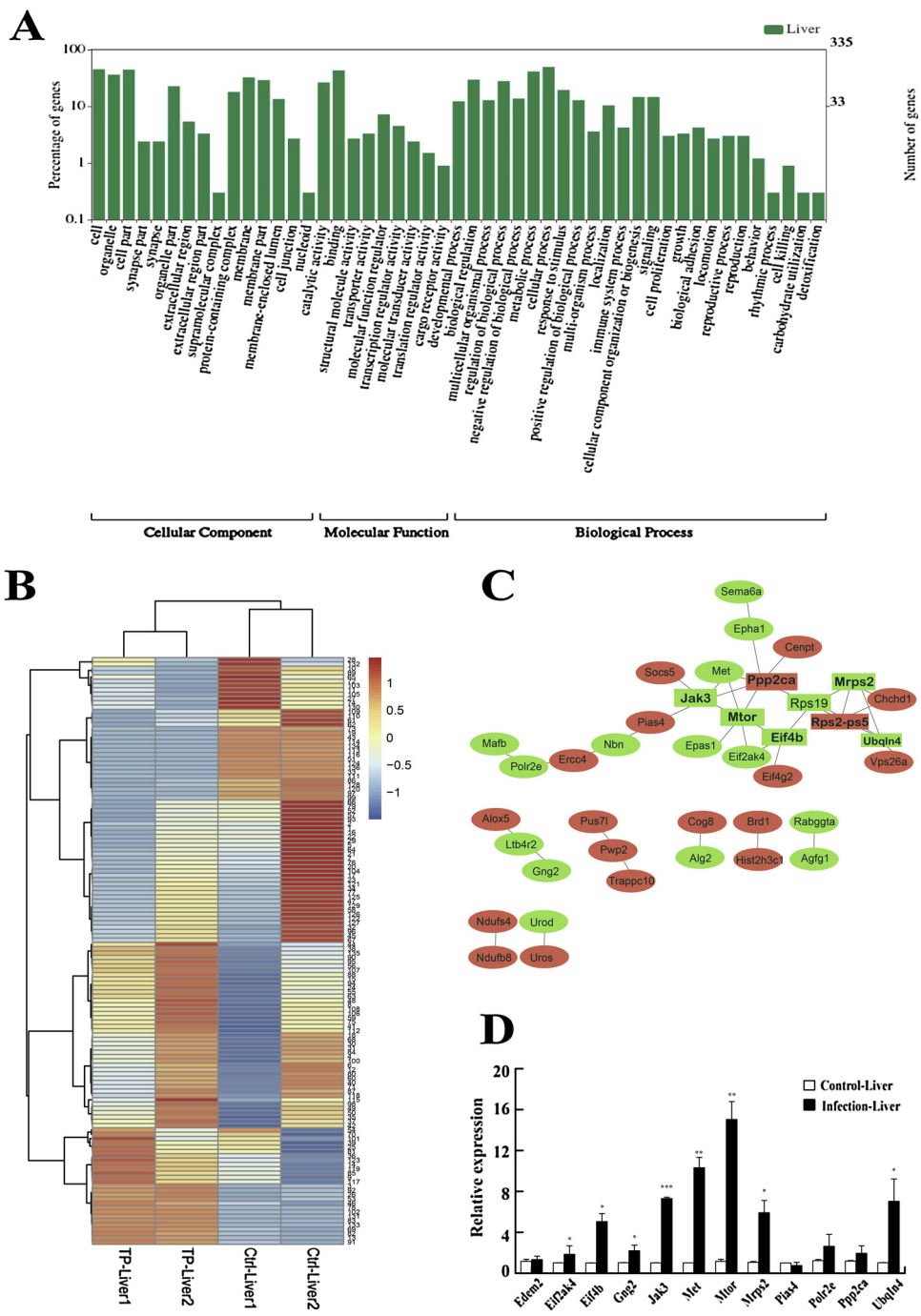

Fig. 1. Comparative transcriptome analysis for the DEGs of mice liver after infection with *T. pyogenes*. (A) Each annotated sequence was assigned at least one GO term in three main categories (biological process, cellular component and molecular function), and 49 subcategories. The x-axis represents the GO term; the y-axis denotes the number of proteins. (B) The hierarchical clustering analysis was performed for the DEGs of mice liver. Red and blue colors indicate up- and down- regulated DEGs in the liver, respectively. (C) The PPI network of the DEGs in mice liver was constructed. Red and green circles represent down-regulated and up-regulated genes in the mice liver, respectively. The pane indicates the key nodes. (D) The interested genes that were differentially expressed between the control and infected liver samples were verified by quantitative PCR. The livers were collected as described in methods. Control-siRNA treated samples was used as a control. Data from qPCR were calculated by using the $2^{-\triangle CT}$ method and normalized *β-actin* levels. Data are shown as the mean ± SEM of three independent experiments. $*p <$ 0.05, $**p <$ 0.01 and $***p < 0.001$. (For interpretation of the references to colour in this figure legend, the reader is referred to the web version of this article).

increased CFU in RAW264.7 cells following infection. These findings implied that autophagy may play a key role in the regulation of *T. pyogenes* elimination.

3.3. The mTOR siRNA treatment of murine macrophages reduced bacterial burdens

To further investigate whether *T. pyogenes* could be eliminated by inhibiting mTOR, RAW264.7 were transfected control or mTOR siRNA for 24 h and infected with *T. pyogenes* TP8 at an MOI of 10 for 6 h. As shown in Fig. 3A, bacterial CFU increased significantly in the RAW264.7 treated with NC siRNA, whereas transfection with mTOR siRNA partially reversed these effects with decreased CFU in *T. pyogenes*-infected cells. The result was further confirmed by using another isolates TP7 and TP13. We then analyzed the induction of autophagosomal membrane-associated protein LC3 by inhibited mTOR in macrophages using confocal microscopy. Our results showed that transfection with mTOR siRNA induced autophagy with LC3 puncta in RAW264.7 cells (Fig. 3B). In addition, we further performed immunoblotting to determine the expression patterns of LC3, which is an important marker of microtubule-associated protein in the autophagosomal membrane in the RAW264.7 cells. Western blotting analysis indicated that mTOR siRNA significantly reduced mTOR expression and induced endogenous conversion of LC3-I to LC3-II in RAW264.7 cells following *T. pyogenes* infection (Fig. 3C). However, the total amount of LC3 and the ratio changes was not significantly altered in the NC siRNA-treated group (Fig. 3C). Similarly, the qPCR results showed that the expression of mTOR (> 75% knockdown as determined as Fig. S1E shown) or S6K1 was reduced and the expression of LC3 or 4EBP1 was increased in the cells transfected with mTOR siRNA after *T. pyogenes*

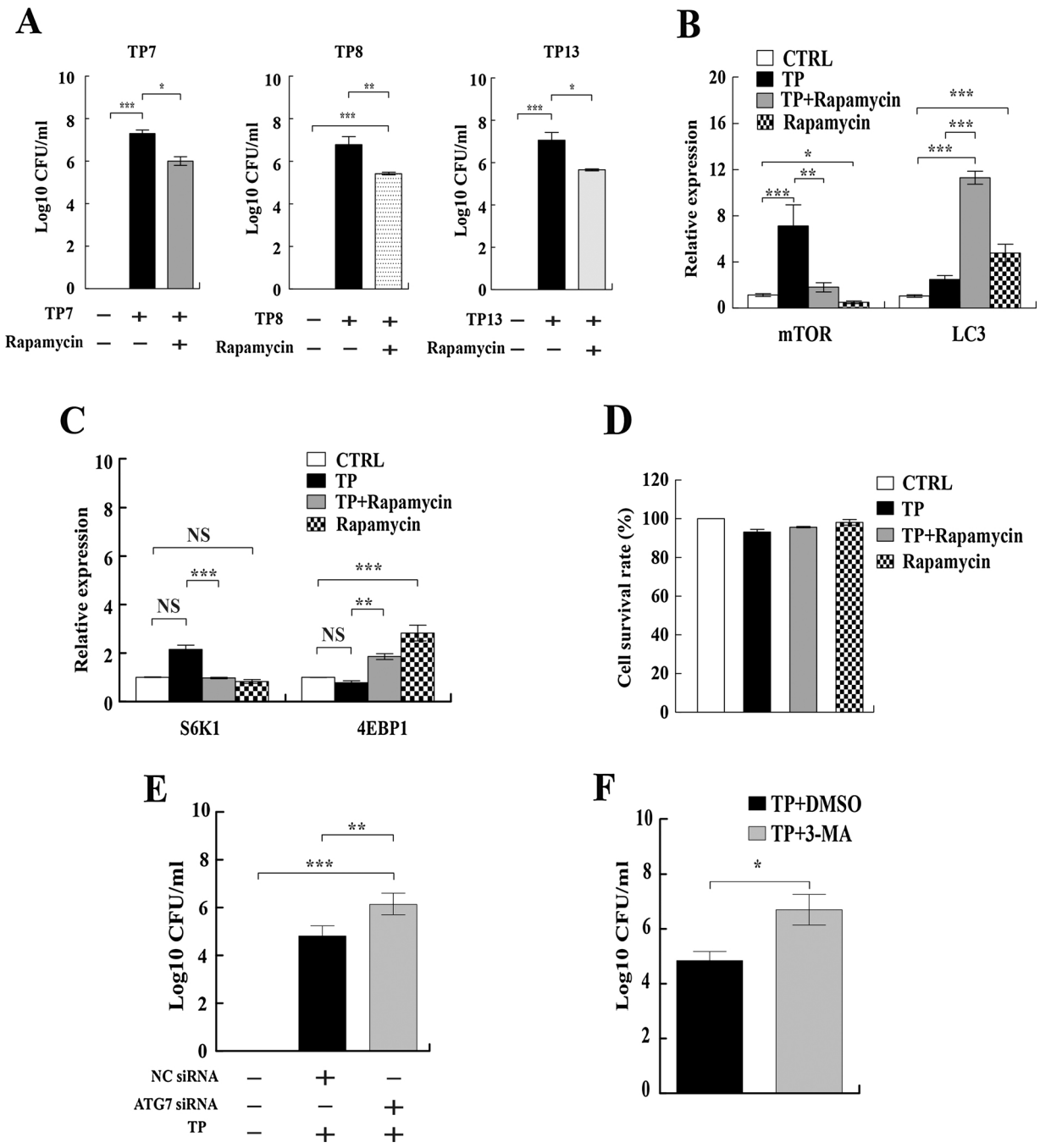

Fig. 2. Rapamycin treatment of murine macrophages induced autophagy and reduced bacterial burdens. (A) RAW264.7 were infected with *T. pyogenes* TP7/TP8/TP13 at an MOI of 10 for 6 h, and treated with rapamycin (100 nM) for 3 h. After extracellular bacteria were killed by gentamicin treatment, RAW264.7 cells were lysed and the intracellular bacteria on the BHI agar plates were counted. The expression levels of mTOR and LC3 were detected by qPCR (B). The expression levels of S6K1 and 4EBP1 were detected by qPCR (C). (D) The cell viability was detected by MTT assay. (E) RAW264.7 were transfected control or ATG7 siRNA for 24 h and infected with *T. pyogenes* at an MOI of 10 for 6 h. The bacterial burdens were determined as described above. (F) RAW264.7 were infected with *T. pyogenes* at an MOI of 10 for 6 h and treated with DMSO or 3-MA (5 μM) for 3 h. The bacterial burdens were determined as described above. Data are shown as the mean ± SEM of three independent experiments. $^{***}p < 0.001$, $^{**}p < 0.01$, $^{*}p < 0.05$.

infection (Fig. 3D and E). The cell survival of RAW264. 7 cells were also slightly improved by treated with mTOR siRNA during *T. pyogenes* infection (Fig. 3F). However, transient transfection with a plasmid expressing mTOR effectively increased the viability of *T. pyogenes* in RAW264.7 cells compared to treatment with the control plasmid (Fig. 3G). Taken together, these results suggested that mTOR functions as potent regulators in autophagy-mediated *T. pyogenes* elimination.

3.4. The inhibition of mTOR regulated oxidation and cytokines against T. pyogenes in murine macrophages

Previous studies have demonstrated that autophagy could be stimulated to clear reactive oxygen species (ROS) and to protect cells by combating bacterial toxin-induced damage (Li et al., 2015a; Yuan et al., 2009). To explore the effect of inhibition of mTOR on the host in response to *T. pyogenes* infection, the infected RAW264.7 cells were collected after treated with rapamycin. As determined by NBT assay

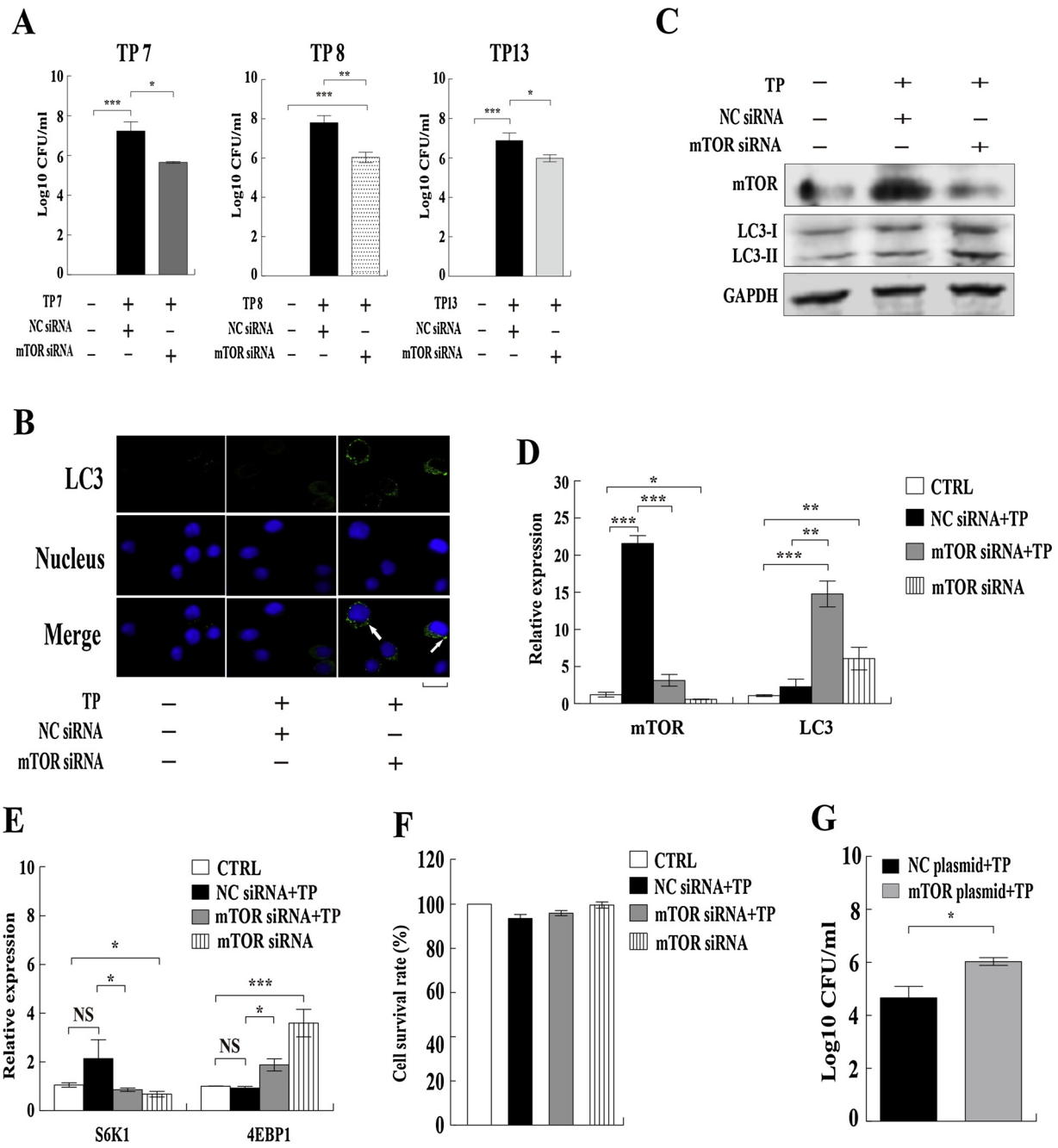

Fig. 3. The mTOR siRNA treatment of murine macrophages reduced bacterial burdens. (A) RAW264.7 were transfected control or mTOR siRNA for 24 h–48 h and infected with *T. pyogenes* TP7/TP8/TP13 at an MOI of 10 for 6 h. The bacterial burdens were determined as described in Fig. 2. (B) RAW264.7 cells were fixed and then immunostained with mouse anti-LC3 antibody followed by Alexa Fluor 488-conjugated goat anti-mouse IgG antibody (green). The localization of LC3 was detected by confocal microscopy. Arrows indicate the localization of LC3; scale bar, 20 μm. The expression levels of mTOR and LC3 were detected by western blotting (C) and qPCR (D). The expression levels of S6K1 and 4EBP1 were detected by qPCR (E). (F) The cell viability was detected by MTT assay. (G) RAW264.7 were transfected NC or mTOR plasmids for 24 h and infected with *T. pyogenes* at an MOI of 10 for 6 h. The bacterial burdens were determined as described above. Data are shown as the mean ± SEM of three independent experiments. ***$p < 0.001$, **$p < 0.01$ and *$p < 0.05$. (For interpretation of the references to colour in this figure legend, the reader is referred to the web version of this article).

(Fig. 4A), the oxidative stress was declined in rapamycin-treated cells compared to *T. pyogenes*-infected cells. This result was confirmed by H_2DCF assay that quantifies superoxide (Fig. 4B). Moreover, mitochondrial membrane potential was decreased in cells infected with *T. pyogenes*, as determined by using the JC-1 fluorescence assay (Fig. 4C). To further confirm the effect of eliminating bacterium by decreased ROS, the RAW264.7 cells were infected with *T. pyogenes* for 6 h, and treated with rapamycin and NAC (*N*-acetyl-L-cysteine), a well-known inhibitor of ROS for 3 h. As indicated by CFU data (Fig. 4D), treating both with rapamycin and NAC significantly reduced the viability of *T. pyogenes* in RAW264.7.

The proinflammatory cytokines function as the key mediators in response to bacterial inflammation. To further study the host inflammatory responses against *T. pyogenes* infection by inhibiting mTOR, the infected cells were collected after treated as above. The results showed that the relative levels of TNF-α, IL-1β, and IL-6 in the RAW264.7 were decreased when treated with mTOR siRNA by qPCR (Fig. 4E) and ELISA (Fig. 4F). No obvious changes of TNF-α, IL-1β, IL-6

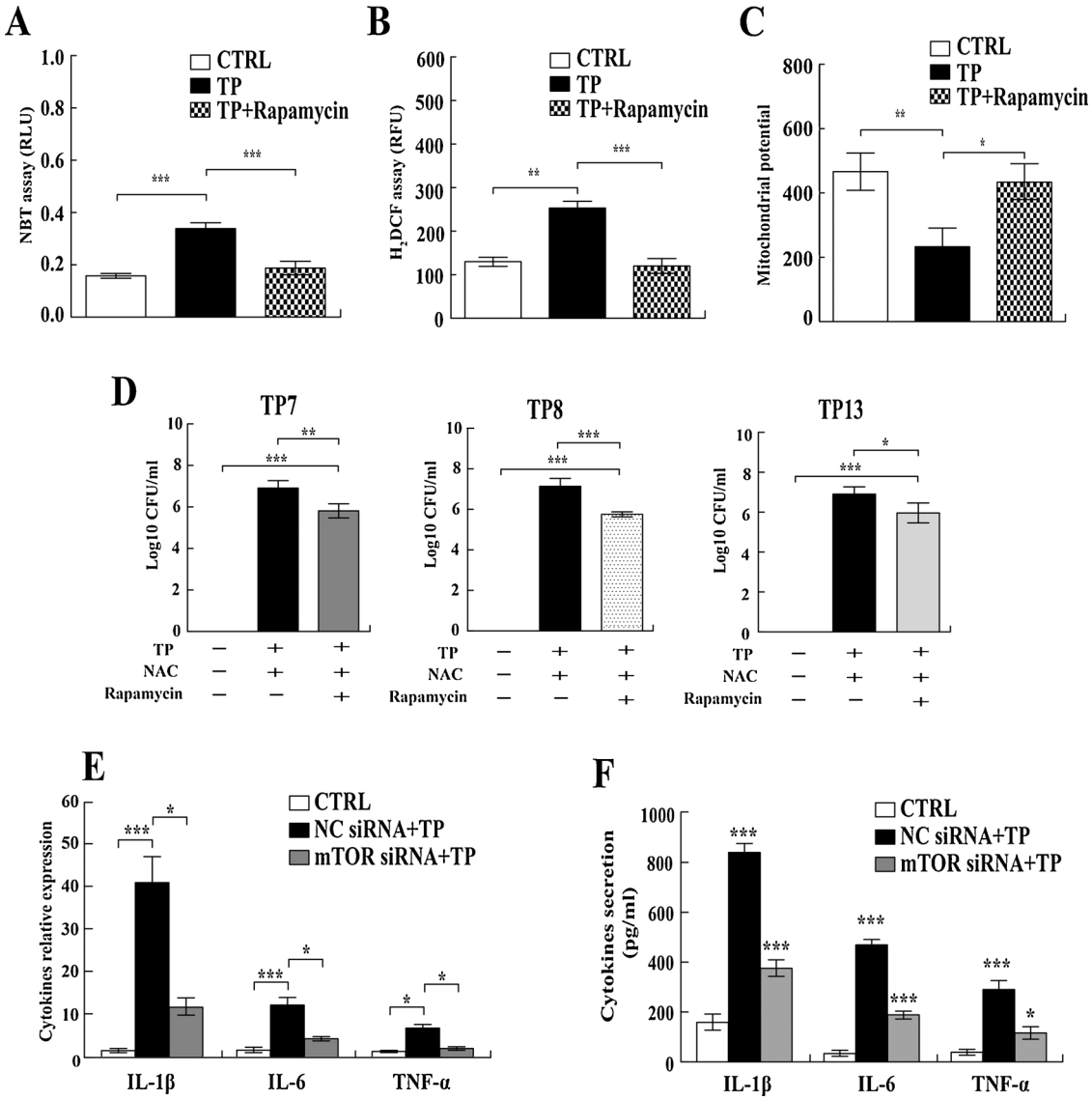

Fig. 4. The inhibition of mTOR regulated ROS and cytokines against *T. pyogenes* in murine macrophages. (A–D) RAW264.7 were infected with *T. pyogenes* TP8 at an MOI of 10 for 6 h, and treated with rapamycin or NAC (3 mM) for 3 h. Superoxide production in MH-S cells was detected by an NBT assay at a wavelength of 560 nm (A) and an H_2DCF assay at a wavelength of 488 nm (B). Mitochondrial potential of MH-S cells was measured by the JC-1 fluorescence assay at a wavelength of 532 nm (C). The bacterial burdens (TP7/TP8/TP13) were determined as described previously in Fig. 3 (D). (E and F) RAW264.7 were transfected control or mTOR siRNA for 24 h and infected with *T. pyogenes* at an MOI of 10 for 6 h. The levels of IL-1β, IL-6 and TNF-α were detected by qPCR (E) and ELISA assays (F). Data are shown as the mean ± SEM of three independent experiments. *, $p < 0.05$; **, $p < 0.01$; ***, $p < 0.001$.

were detected in the control group. Taken together, these findings suggested that inhibition of mTOR regulated the oxidation and the expression of pro-inflammatory cytokines to respond *T. pyogenes* infection.

3.5. The inhibition of mTOR protected mice against T. pyogenes challenge

To investigate the ability of mTOR inhibition-raised immune responses to eliminate *T. pyogenes* infection *in vivo*, the bacterial burdens in the liver or PF of mice were measured after intraperitoneal challenge with *T. pyogenes* TP8. The results showed that an amounts of bacteria were detected from the liver and PF of control siRNA-treated mice. However, the mice treated with mTOR siRNA displayed fewer bacteria in the liver (Fig. 5A) and PF (Fig. 5B). As shown in Fig. 5C, control siRNA-treated mice died at 7 days post infection (dpi). In contrast, almost half of the mice treated with mTOR siRNA survived the *T. pyogenes* challenge at 14 dpi (Fig. 5C). Additionally, a necrotic center containing cellular debris, leukocytes or hepatocytes were observed in the mice livers of control group (Fig. 5D). Compared to control group, the mTOR siRNA (Fig. 5D) treated mice remarkably eliminated invading *T. pyogenes* in their livers and the liver tissue had less pathological changes. Altogether, these results suggest that inhibition of mTOR effectively protected mice from *T. pyogenes* challenge.

4. Discussion

In the past few decades, *T. pyogenes* has been demonstrated as an important cause of different clinical manifestations in livestock (Ribeiro et al., 2015), and thus our research is of particular importance for domestic animal husbandry. Next-generation sequencing technology provides large-scale genomic resources and useful details on the underlying pathogenic mechanisms following the microorganism infection (Villarino et al., 2017). In the present study, we used *T. pyogenes* TP8 infected liver samples of mice to perform a genome-wide investigation by transcriptional sequencing and mRNA expression profile analysis. A total of 136 DEGs were identified in the liver infected samples

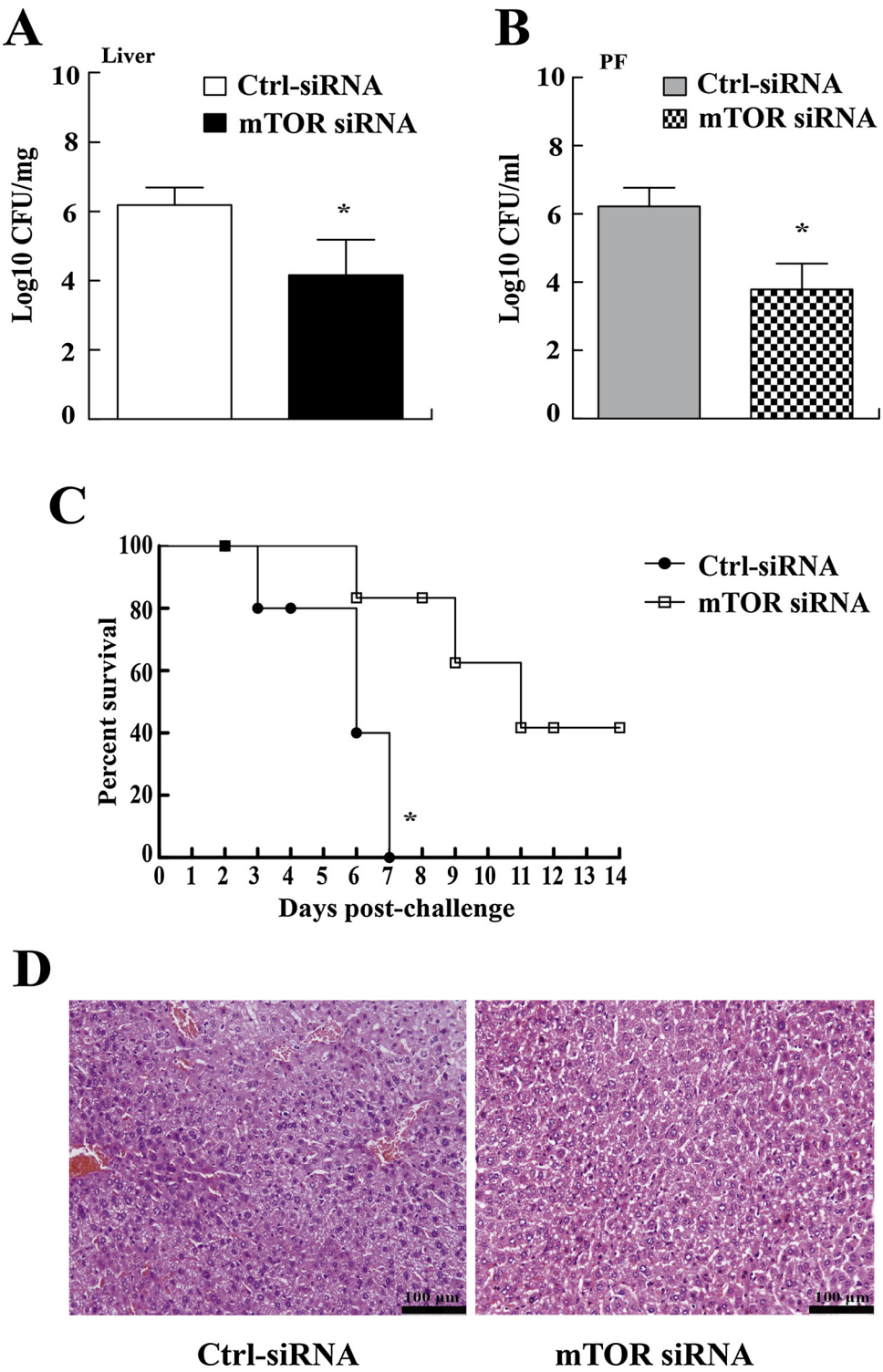

Fig. 5. Residual CFUs, survival rate, and histological analysis of mice challenged intraperitoneally with *T. pyogenes*. (A–D) Mice were treated with ctrl-siRNA or mTOR siRNA as described in methods. The mice were intraperitoneally challenged at day 3 with 3.7×10^7 CFU *T. pyogenes* TP8. The bacterial burdens of liver (A) and PF (B) were determined at day 2 post-challenge. Survival rate was monitored for the subsequent 14 days (C). The livers of two groups' challenged mice were collected for evaluation of histology alteration (D). Ctrl-siRNA were used as the control. *$p < 0.05$.

compared to normal samples, which demonstrated a functional distribution of GO categories and implied the sequence diversity of this liver transcriptome. Hierarchical clustering analyses provided the comprehensive landscape of the host transcriptome. These findings suggested that *T. pyogenes* infection might be associated with many DEGs, which are likely to play a role in cell invasion and regulation of the host immune system.

To elucidate the signal pathways and DEGs involved in host responses to *T. pyogenes* infection, the KEGG pathway-based and PPI networks analysis was performed to further investigate the DEGs functions and interactions. Among the 11 KEGG pathways that obtained DEGs between infected and control samples in liver were assigned, we found that "metabolic pathways" represented the largest category in liver transcriptome, followed by "PI3K-Akt signaling pathway",

"pathways in cancer," and "Jak-STAT signaling pathway" (Villarino et al., 2017), implying that *T. pyogenes* might affect the host by altering the host cell microenvironment for their own benefit. While a greater number of transcripts were assigned to metabolic processes than the immune system, most of the pathways in signal transduction are involved in and probably play important roles in the immune system, such as PI3K-Akt and mTOR signaling pathways (Saxton and Sabatini, 2017). Additionally, we found that Ppp2ca, Rps19, Jak3, and Mtor had higher betweenness values and degrees in the PPI network, suggesting that these proteins may interact with each other in their own PPI network.

In the current study, the mRNA level of mTOR were significantly augmented in the infected mice compared to the control group. A possible explanation is that *T. pyogenes* invasion might inhibit host autophagy to survive in the host cells by up-regulating mTOR expression. The previous reports demonstrated that *T. pyogenes* was able to survive within host phagocytes such as macrophages (Jost and Billington, 2005). Additionally, the mTOR was a key regulator of autophagy (Jung et al., 2010) and was located in the most significant signaling pathway in this study. Thus, we hypothesized that mTOR may play an essential role in modulating the autophagy process during *T. pyogenes* infection and further investigated its roles throughout this study. As a hub gene in the liver transcriptome, *mtor* coded an evolutionarily conserved protein in the eukaryotic species and functions as a critical regulator in protein synthesis, autophagy, and manipulates the progress of cancer and diabetes (Saxton and Sabatini, 2017). To explore whether autophagy induction could reduce *T. pyogenes* burdens in macrophages, RAW264.7 murine macrophages were infected with *T. pyogenes* and then treated with rapamycin. We found that treatment with rapamycin induced autophagy and increased bacterial elimination in cells. However, blocking autophagy with ATG7 siRNA or autophagy inhibitor 3-MA partially reversed these effects with increased CFU in cells following *T. pyogenes* infection. In agreement with these findings, other reports have indicated that autophagy enhanced bacterial elimination and played a key role in immune defense against pathogen invasion (Li et al., 2015b; Yuan et al., 2012). Mechanistically, the inhibition of mTOR regulated oxidation and cytokines expression such as IL-1β against *T. pyogenes* in murine macrophages by using mTOR siRNA or rapamycin. Indeed, the activation of autophagy by rapamycin could decrease bacterial toxin-mediated ROS production and protect cells against the toxin-caused impairment (Yuan et al., 2009). These interactions in the molecular level might determine the response mechanisms of the host that are necessary to defeat *T. pyogenes* invasions. More importantly, to inhibit mTOR expression significantly protected mice against *T. pyogenes* challenge and increased mice survival rate, which suggested mTOR might be a novel target to control *T. pyogenes* related diseases. These data also imply that *T. pyogenes* might alter the defense responses of the host at the transcriptomic level by increasing expression levels of immune-related and antibacterial defense-related genes and might subsequently impair the immune functions of the host. Taken together, these findings provide a global overview of the pathways and DEGs involved in the immune defense responses of mice during *T. pyogenes* infection.

In summary, we identified numerous immune-associated DEGs and signal pathways by differentially expressed analysis in mice transcriptome following infection with *T. pyogenes*. We found that mTOR is a potent functional regulator involved in immune defense responses with *T. pyogenes* infection. More importantly, our findings are the first to pinpoint the role of autophagy that could protect mice from *T. pyogenes* challenge by inhibiting the expression of mTOR. Overall, this study provides the first informative reference dataset for future studies on global and specific response to *T. pyogenes* infection at the molecular level. It might also facilitate biomarker identification or gene discovery for prevention and control of *T. pyogenes*-related diseases.

Acknowledgements

This work was supported by the Talent Introduction of Project of Chengdu University (2081918021), National Key Programme of Research and Development, Ministry of Science and Technology (2016YFC0503200), Collaboration and Innovation on New Antibiotic Development and Industrialization (2016-XT00-00023-GX from Science and Technology Bureau of Chengdu), and the Sichuan Science and Technology Program (2018HH0007). We thank Dr. Megan Price (Sichuan University) for editing the manuscript.

Appendix A. Supplementary data

Supplementary material related to this article can be found, in the online version, at doi:https://doi.org/10.1016/j.vetmic.2019.06.021.

References

Amos, M.R., Healey, G.D., Goldstone, R.J., Mahan, S.M., Anna, D., Hans-Joachim, S., Olivier, S., Peter, Z., Isabelle, D.L., Smith, D.G.E., 2014. Differential endometrial cell sensitivity to a cholesterol-dependent cytolysin links *Trueperella pyogenes* to uterine disease in cattle. Biol. Reprod. 90, 54.

Damron, F.H., Oglesby-Sherrouse, A.G., Wilks, A., Barbier, M., 2016. Dual-seq transcriptomics reveals the battle for iron during *Pseudomonas aeruginosa* acute murine pneumonia. Sci. Rep. 6, 39172.

Deretic, V., Saitoh, T., Akira, S., 2013. Autophagy in infection, inflammation, and immunity. Nat. Rev. Immunol. 13, 722.

Foldenauer, M.E.B., Mcclellan, S.A., Berger, E.A., Hazlett, L.D., 2013. mTOR regulates IL-10 and resistance to *Pseudomonas aeruginosa* corneal infection. J. Immunol. 190, 5649.

Gomes, L.C., Dikic, I., 2014. Autophagy in antimicrobial immunity. Mol. Cell 54, 224–233.

Haritani, M., Nakazawa, M., Hashimoto, K., Narita, M., Tagawa, Y., Nakagawa, M., 1990. Immunoperoxidase evaluation of the relationship between necrotic lesions and causative bacteria in lungs of calves with naturally acquired pneumonia. Am. J. Vet. Res. 51, 1975–1979.

Huang, T., Song, X., Jing, J., Zhao, K., Shen, Y., Zhang, X., Yue, B., 2018a. Chitosan-DNA nanoparticles enhanced the immunogenicity of multivalent DNA vaccination on mice against *Trueperella pyogenes* infection. J. Nanobiotechnology 16, 8.

Huang, T., Song, X., Zhao, K., Jing, J., Shen, Y., Zhang, X., Yue, B., 2018b. Quorum-sensing molecules N -acyl homoserine lactones inhibit *Trueperella pyogenes* infection in mouse model. Vet. Microbiol. 213, 89–94.

Huang, T., Zhao, K., Zhang, Z., Tang, C., Zhang, X., Yue, B., 2016. DNA vaccination based on pyolysin co-immunized with IL-1β enhances host antibacterial immunity against *Trueperella pyogenes* infection. Vaccine 34, 3469–3477.

Jost, B.H., Billington, S.J., 2005. Arcanobacterium pyogenes: molecular pathogenesis of an animal opportunist. Antonie Van Leeuwenhoek 88, 87–102.

Jung, C., Ro, S., Cao, J., Otto, N., Kim, D., 2010. mTOR regulation of autophagy. FEBS Lett. 584, 1287–1295.

Kolde, R., 2015. Pheatmap: Pretty Heatmaps. R Package Version 1.0. 8.

Lee, D.F., Kuo, H.P., Chen, C.T., Hsu, J.M., Chou, C.K., Wei, Y., Sun, H.L., Li, L.Y., Ping, B., Huang, W.C., 2007. IKK beta suppression of TSC1 links inflammation and tumor angiogenesis via the mTOR pathway. Cell 130, 440–455.

Li, P., Shi, J., He, Q., Hu, Q., Wang, Y.Y., Zhang, L.J., Chan, W.T., Chen, W.X., 2015a. Streptococcus pneumoniae induces autophagy through the inhibition of the PI3K-I/Akt/mTOR pathway and ROS hypergeneration in A549 cells. PLoS One 10, e0122753.

Li, R., Tan, S., Yu, M., Jundt, M., Zhang, S., Wu, M., 2015b. Annexin A2 regulates autophagy in *Pseudomonas aeruginosa* infection through the Akt1-mTOR-ULK1/2 signaling pathway. J. Immunol. 195, 3901–3911.

Liu, M., Xing, Y., Zhang, D., Guo, S., 2015. Transcriptome analysis of genes involved in defence response in Polyporus umbellatus with *Armillaria mellea* infection. Sci. Rep. 5.

Liu, Q., Miller, L.C., Blecha, F., Sang, Y., 2017. Reduction of infection by inhibiting mTOR pathway is associated with reversed repression of type I interferon by porcine reproductive and respiratory syndrome virus. J. Gen. Virol. 98, 1316–1328.

Martin, J.A., Wang, Z., 2011. Next-generation transcriptome assembly. Nat. Rev. Genet. 12, 671–682.

Pertea, M., Kim, D., Pertea, G.M., Leek, J.T., Salzberg, S.L., 2016. Transcript-level expression analysis of RNA-seq experiments with HISAT, StringTie and Ballgown. Nat. Protoc. 11, 1650–1667.

Pertea, M., Pertea, G.M., Antonescu, C.M., Chang, T.-C., Mendell, J.T., Salzberg, S.L., 2015. StringTie enables improved reconstruction of a transcriptome from RNA-seq reads. Nat. Biotechnol. 33, 290–295.

Preta, G., Lotti, V., Cronin, J.G., Sheldon, I.M., 2015. Protective role of the dynamin inhibitor dynasore against the cholesterol-dependent cytolysin of *Trueperella pyogenes*. Faseb J. 29, 1516–1528.

Ribeiro, M., Risseti, R., Bolaños, C., Caffaro, K., de Morais, A., Lara, G., Zamprogna, T., Paes, A., Listoni, F., Franco, M., 2015. *Trueperella pyogenes* multispecies infections in domestic animals: a retrospective study of 144 cases (2002 to 2012). Vet. Q. 35,

82–87.
Saito, R., Smoot, M.E., Ono, K., Ruscheinski, J., Wang, P.-L., Lotia, S., Pico, A.R., Bader, G.D., Ideker, T., 2012. A travel guide to Cytoscape plugins. Nat. Methods 9, 1069–1076.
Sato, T., Nakashima, A., Guo, L., Coffman, K., Tamanoi, F., 2010. Single amino-acid changes that confer constitutive activation of mTOR are discovered in human cancer. Oncogene 29, 2746–2752.
Saxton, R.A., Sabatini, D.M., 2017. mTOR signaling in growth, metabolism, and disease. Cell 168, 960–976.
Villarino, A.V., Kanno, Y., O'Shea, J.J., 2017. Mechanisms and consequences of Jak-STAT signaling in the immune system. Nat. Immunol. 18, 374–384.
Yang, Z., Klionsky, D.J., 2010. Mammalian autophagy: core molecular machinery and signaling regulation. Curr. Opin. Cell Biol. 22, 124–131.
Young, M.D., Wakefield, M.J., Smyth, G.K., Oshlack, A., 2010. Gene ontology analysis for RNA-seq: accounting for selection bias. Genome Biol. 11, R14.
Yuan, H., Perry, C.N., Huang, C., Iwai-Kanai, E., Carreira, R.S., Glembotski, C.C., Gottlieb, R.A., 2009. LPS-induced autophagy is mediated by oxidative signaling in cardiomyocytes and is associated with cytoprotection. Am. J. Physiol. Heart Circ. Physiol. 296, H470.
Yuan, K., Huang, C., Fox, J., Laturnus, D., Carlson, E., Zhang, B., Yin, Q., Gao, H., Wu, M., 2012. Autophagy plays an essential role in the clearance of *Pseudomonas aeruginosa* by alveolar macrophages. J. Cell. Sci. 125, 507–515.
Zhao, K., Li, W., Huang, T., Song, X., Zhang, X., Yue, B., 2017. Comparative transcriptome analysis of *Trueperella pyogenes* reveals a novel antimicrobial strategy. Arch. Microbiol. 199, 649–655.
Zhao, K., Li, W., Kang, C., Du, L., Huang, T., Zhang, X., Wu, M., Yue, B., 2014. Phylogenomics and evolutionary dynamics of the family *Actinomycetaceae*. Genome Biol. Evol. 6, 2625–2633.
Zhao, K., Liu, Y., Zhang, X., Wang, H., Yue, B., 2011. Detection and characterization of antibiotic-resistance genes in *Arcanobacterium pyogenes* strains from abscesses of forest musk deer. J. Med. Microbiol. 60, 1820–1826.
Zhao, K., Tian, Y., Yue, B., Wang, H., Zhang, X., 2013. Virulence determinants and biofilm production among *Trueperella pyogenes* recovered from abscesses of captive forest musk deer. Arch. Microbiol. 195, 203–209.
Zhou, C., Elsheikha, H., Zhou, D., Liu, Q., Zhu, X., Suo, X., 2016. Dual identification and analysis of differentially expressed transcripts of porcine PK-15 cells and *Toxoplasma gondii* during in vitro Infection. Front. Microbiol. 7, 721.